

Characterization of a Protein-based Adhesive Elastomer Secreted by the Australian Frog *Notaden bennetti*

Lloyd D. Graham,^{*,†} Veronica Glattauer,[‡] Mickey G. Huson,[§] Jane M. Maxwell,[§] Robert B. Knott,^{||} John W. White,[⊥] Paul R. Vaughan,[‡] Yong Peng,[‡] Michael J. Tyler,[#] Jerome A. Werkmeister,[‡] and John A. Ramshaw[‡]

CSIRO Molecular & Health Technologies, Sydney Laboratory, P.O. Box 184, North Ryde, NSW 1670, Australia, CSIRO Molecular & Health Technologies, Ian Wark Laboratory, Bag 10, Clayton South, Victoria 3169, Australia, CSIRO Textile & Fibre Technology, P.O. Box 21, Belmont, Victoria 3216, Australia, Australian Nuclear Science and Technology Organisation, Menai, NSW 2234, Australia, Research School of Chemistry, Australian National University, Canberra, ACT 0200, Australia, and School of Earth & Environmental Sciences, University of Adelaide, South Australia 5005, Australia

Received May 15, 2005; Revised Manuscript Received June 29, 2005

When provoked, *Notaden bennetti* frogs secrete an exudate which rapidly forms a tacky elastic solid (“frog glue”). This protein-based material acts as a promiscuous pressure-sensitive adhesive that functions even in wet conditions. We conducted macroscopic tests in air to assess the tensile strength of moist glue (up to 78 ± 8 kPa) and the shear strength of dry glue (1.7 ± 0.3 MPa). We also performed nanomechanical measurements in water to determine the adhesion (1.9–7.2 nN or greater), resilience (43–56%), and elastic modulus (170–1035 kPa) of solid glue collected in different ways. Dry glue contains little carbohydrate and consists mainly of protein. The protein complement is rich in Gly (15.8 mol %), Pro (8.8 mol %), and Glu/Gln (14.1 mol %); it also contains some 4-hydroxyproline (4.6 mol %) but no 5-hydroxylysine or 3,4-dihydroxyphenylalanine (L-Dopa). Denaturing gel electrophoresis of the glue reveals a characteristic pattern of proteins spanning 13–400 kDa. The largest protein (Nb-1R, apparent molecular mass 350–500 kDa) is also the most abundant, and this protein appears to be the key structural component. The solid glue can be dissolved in dilute acids; raising the ionic strength causes the glue components to self-assemble spontaneously into a solid which resembles the starting material. We describe scattering studies on dissolved and solid glue and provide microscopy images of glue surfaces and sections, revealing a porous interior that is consistent with the high water content (85–90 wt %) of moist glue. In addition to compositional similarities with other biological adhesives and well-known elastomeric proteins, the circular dichroism spectrum of dissolved glue is almost identical to that for soluble elastin and electron and scanning probe microscopy images invite comparison with silk fibroins. Covalent cross-linking does not seem to be necessary for the glue to set.

Introduction

Australian frogs of the genus *Notaden* secrete a sticky material on their backs when they are provoked, probably in an attempt to deter potential predators.¹ The exudate sets rapidly as a yellow-colored tacky elastic solid (“frog glue”), and this protein-based material acts as a promiscuous pressure-sensitive adhesive. Although the frogs are land-based animals, spending much of their time underground, they emerge to breed after flooding rains and the glue functions even in wet conditions. Initial laboratory tests have shown that the material adheres tightly and with comparable affinity to a wide variety of surfaces such as glass, metal,

wood, cardboard, and plastic (including polypropylene, polystyrene, and even the nonstick polymer poly(tetrafluoroethylene)).² Preliminary tests in vitro and in vivo indicate that the natural glue can also be used to bond and repair biological tissues,³ suggesting that, in due course, it may be possible to use a chemical or recombinant mimic of this material as a novel medical adhesive. Such a product would be valuable as there is a significant unmet clinical need for a strong and flexible surgical glue that is highly biocompatible.⁴ Current biological adhesives (fibrin, albumin, gelatin-resorcinol-formaldehyde, etc.) suffer from low bond strength and are in some cases derived from blood products, with associated risk of viral or prion contamination. On the other hand, synthetic glues (e.g., cyanoacrylate adhesives) are very strong but they are also toxic to living tissues and form rigid, nonporous films that can hinder wound healing.

In this article we report procedures by which the glue produced by the frog *Notaden bennetti* can be collected and manipulated. We characterize its material properties, describe

* Corresponding author. Phone: +61 2 9490 5003. Fax: +61 9490 5010. E-mail: lloyd.graham@csiro.au.

[†] CSIRO Molecular & Health Technologies, Sydney Laboratory.

[‡] CSIRO Molecular & Health Technologies, Ian Wark Laboratory.

[§] CSIRO Textile & Fibre Technology.

^{||} Australian Nuclear Science and Technology Organisation.

[⊥] Australian National University.

[#] University of Adelaide.

its composition and structure, propose a mechanism for its solidification, and identify similarities with other biomaterials. The data we present for this unusual natural product should be of value not only to naturalists concerned with the biology of amphibia but also to those interested in the development and application of new biomedical materials.

Experimental Section

Glue Collection. *N. bennetti* frogs were captured from private land under permit in rural Queensland and maintained in culture. To collect the glue, frogs' backs were rinsed clean with distilled water and the dermal musculature stimulated electrically as described previously.⁵ The pH of fresh exudate was established using indicator sticks (Merck). In most cases the exudate was collected under irrigation with buffer solutions as specified in the Results section, where the different types of solid glue (types I–III) are defined fully. (To distinguish the set glue from liquid forms and fractions we refer to it as a solid, although strictly speaking it is a hydrogel.) Briefly, type I glue was produced by emulsifying the secretion by irrigation with phosphate-buffered saline (PBS)/10 mM Cys·HCl, pH 4.5, and collecting the sticky yellow material that settled out on standing. The other glue types were the rubbery yellow solids that accumulated directly around the probe during collections done in the absence of an emulsifying irrigant. Thus, type II glue denotes material that solidified around the electrode during irrigation with water or 20 mM phosphate buffer, pH 6.2, and type III glue indicates material that solidified around the electrode in the absence of any irrigation. PBS was 10 mM phosphate buffer containing 130 mM NaCl and 2.7 mM KCl, pH 7.4. All samples were collected in an argon-filled chamber except where 20 mM phosphate buffer, pH 6.2, was used as irrigant. Samples of solid glue that were stored at -70°C in their cognate washings (if any) appeared to retain all the functionality of the unfrozen solid.

Macroscopic Strength Tests. Tensile tests of polypropylene bonded by moist glue made use of plungers from 1 mL tuberculin syringes (Terumo) whose thumb-disks (1 cm diameter) had been sanded with P1200-grade abrasive paper, rinsed in ethanol, and air-dried before use. For polypropylene bonded by freshly secreted exudate, undiluted frog secretion was collected directly onto one of the thumb-disks and immediately sandwiched between a second disk with firm hand pressure. For polypropylene bonded by type I glue, a suitably sized piece of solid glue was removed from solution and sandwiched between two thumb-disks with firm hand pressure, using a reciprocating motion (in the plane of the disks) to ensure optimal engagement of the glue with the surface. Tensile strength tests of the thumb-disk joints were done in air at room temperature using either a simple test rig (in which glass or lead shot was added slowly to a container attached to the lower plunger until the joint failed) or an Instron model 5567 equipped with a ± 1 kN static load cell and a cross-head speed of 50 mm/min. The two methods gave comparable strength values, and in either case each test was completed within 3 min. For lap-shear tests of dry type I glue, pairs of birch-wood craft sticks were lap-jointed by

sandwiching a piece of moist solid glue between a 1 cm overlap and squeezing the sticks together firmly. Test pieces were allowed to dry for 1 week and then tested to failure on an Instron model 5568 using a ± 1 kN static load cell and a cross-head speed of 1 mm/min. After separation, the glued region in each test piece was outlined in ink and its area calculated by image analysis (Image Pro Plus, MediaCybernetics). Reference adhesives were UHU Stic (Article No. 70, UHU GmbH & Co. KG, Bühl, Germany), Blu-Tack (Bostik, Australia), polyvinyl acetate (Craft PVA glue, Educational Colors Ltd., Victoria, Australia), and cyanoacrylate (Selley's SupaGlue, NSW, Australia).

Nanomechanical Measurements. Samples of type I and type III glue were presoaked in water and then examined in clean water using a Digital Instruments Dimension 3000 Scanning Probe Microscope equipped with a silicon nitride probe ($k \approx 0.58$ N/m). To obtain force–distance curves, the probe was initially driven into the glue and then retracted. Modulus calculations, which were based on compression data, assumed that the probe tip was parabolic ($r = 50$ nm) and that the glue behaved as a perfect rubber (Poisson's ratio = 0.5).

Biochemical Composition. For determination of water content, glue pellets were allowed to hydrate fully by standing in water or buffer for at least 24 h. Surface liquid was removed by blotting, and the moist pellets were weighed. After vacuum-drying overnight, the pellets were reweighed. The carbohydrate content of vacuum-dried type I glue was measured colorimetrically using the phenol–sulfuric acid assay⁶ with D-glucose as the standard. The glue dissolved instantly in the assay reagent (final concentration 67% (w/w) sulfuric acid). This assay detects individual aldoses, ketoses, deoxysugars, and sugar acids with somewhat different efficiencies, so results are reported in terms of glucose equivalents. Protein assays of glue solutions (in 5% (v/v) acetic acid) were routinely done by Coomassie Plus (Pierce) using bovine serum albumin (Pierce) for calibration. Quantitative amino acid analysis of type I glue confirmed that the Coomassie-based assay gave protein concentrations that were accurate to $\pm 3\%$. Standard amino acid analyses⁷ involved gas-phase hydrolysis (5.8 M HCl containing 0.2% (w/v) phenol, 108°C , 24 h) followed by HPLC (Waters Alliance instrument equipped with a Waters cation exchange column, cat. Wat080002) with postcolumn ninhydrin detection (Waters 2487 UV/Vis detector) and automatic quantitation (Waters Empower software). Aminoguanidinopropionic acid was used as an internal standard. Analyses for 3,4-dihydroxyphenylalanine (L-Dopa) were similar but employed modified hydrolysis conditions to preserve this residue.⁸ L-Dopa was detected in reference samples with $\sim 90\%$ efficiency. Sodium dodecyl sulfate–polyacrylamide gel electrophoresis (SDS–PAGE) was routinely done using precast Tricine 10–20% gradient gels (Novex) calibrated with BioRad Unstained Precision Plus standards. Unless stated otherwise, samples were boiled for 2 min in sample buffer (final concentration 0.45 M Tris-HCl, pH 8.5, 12% (v/v) glycerol, 4% (w/v) SDS) supplemented with 3% (v/v) 2-mercaptoethanol before loading. Gels were Coomassie-stained using PhastGel Blue R (Pharmacia). The glue proteins

and standards migrate somewhat faster in equivalent gels containing Tris/Glyc buffer (BioRad). Gel filtration chromatography of dissolved type I glue was undertaken using a Pharmacia Superdex-200 HR 10/30 column. Since the column could not tolerate 5% (v/v) acetic acid, it was equilibrated with 45 mM acetic acid containing 4 M urea and 10 mM 2-mercaptoethanol, pH 3.2, a buffer in which type I glue is soluble at ~ 6 mg protein/mL. Other gel filtration separations were attempted using a Waters Ultrahydrogel column equilibrated with 5% (v/v) acetic acid.

Solubilization and Solidification. Rheological characterization of dissolved glue was done as described in the legend to Supporting Information Figure 1b. Poly(ethylene oxide), which was used as a dehydrating agent to solidify the glue from solution, had an average molecular mass of 900 kDa (Aldrich, cat. 18945-6). To compare the resolidification behavior of elastin with that of frog glue, bovine α_2 -elastin (Elastin Products Co.) was dissolved at 7.5 mg/mL 5% (v/v) acetic acid and sufficient 5 M NaCl solution was added to cause a precipitate. The suspension was then centrifuged briefly, and the protein film was harvested by scraping. Tests for thermal coacervation of the frog glue were done by incubating a solution of type I glue (4 mg protein/mL) in 5% (v/v) acetic acid at 40, 60, 80, 99, and 4 °C (15 min each, in sequence) and another (6 mg of protein/mL) in 0.05% (v/v) acetic acid at 40, 60, 80, and 4 °C.

Spectroscopy. Nuclear magnetic resonance (NMR) was used to probe the chemical composition of the frog glue; details are provided in the legend to Supporting Information Figure 2. To investigate the chromophores in the glue, the absorbance spectrum of dissolved type I glue (~ 4 mg of protein/mL in 5% (v/v) acetic acid) was measured in a quartz cuvette by scanning from 190 to 1100 nm in a Shimadzu UV-1601 spectrophotometer with 5% (v/v) acetic acid as the reference sample. For circular dichroism (CD), which gives information about the relative content of different kinds of protein secondary structure, type I glue was dissolved in 10 mM H_3PO_4 at 0.1 mg of protein/mL and the CD spectrum collected using a Jasco J-720 spectrophotometer standardized with camphor sulfonic acid. The spectrum was deconvoluted using a program written by Norma Greenfield (University of Medicine & Dentistry of New Jersey).⁹

Scattering Studies. Radiation scattering potentially provides information about the size and shape of particles (proteins, complexes, micelles, etc.). The techniques used here operate on scales larger than radiation diffraction but smaller than optical microscopy, and encompass the lower end of the size range accessible by transmission electron microscopy (TEM). Thus, small-angle neutron scattering (SANS) and small-angle X-ray scattering (SAXS) operate in the size range from 10^{-9} to 10^{-7} m, while dynamic light scattering (DLS) is more effective in the size range from 10^{-8} to 10^{-6} m. No information about particle shape was obtained in the scattering studies done on frog glue, so particle sizes from SAXS and SANS are reported in terms of a model-independent radius of gyration, R_g (the root-mean-square of the mass-weighted distances of all subvolumes in a particle from its center of mass; for a sphere of radius R , $R_g = 0.775R$) while those from DLS are given in terms of

the hydrodynamic radius, R_h (the particle radius in a hypothetical population of monodisperse hard spheres that would produce the observed scattering). SANS details are provided in the legend to Supporting Information Figure 3. SAXS was done using the camera at the Research School of Chemistry, Australian National University,¹⁰ to study the scattering from dry, moist, and dissolved type I glue samples, in the last instance using glue dissolved at 7.6 mg of protein/mL in 5% (v/v) acetic acid containing 2 mM dithiothreitol. Spherical R_g values were converted to molecular masses (kDa) using published equivalence data.^{11,12} DLS was studied at 25 °C using Malvern HPPS and Zetasizer-nano instruments in General Purpose mode with automatic positioning. Samples were solutions of type I glue dissolved in 5% (v/v) acetic acid at 0.076–0.76 mg of protein/mL in 5% (v/v) acetic acid containing 1.3 mM dithiothreitol. Mean R_h values were converted to molecular masses (kDa) using published equivalence data.^{13–16}

Imaging. Resin-embedded type I glue could not be prepared for TEM because the glue rehydrated when sections were floated off the knife, so samples of reconstituted type I glue (i.e., glue dissolved and resolidified as described below) were smeared on copper grids, air-dried, and imaged using a Philips CM100 microscope. Low-magnification scanning electron microscopy (SEM) was performed using a JEOL JSM-T20 instrument to examine type I glue that had been air-dried and then sputter-coated with gold. High-magnification SEM was performed using a Philips XL30 instrument to examine samples that had been vacuum-dried and then sputter-coated with platinum. For cryoSEM, frozen samples of type I glue were dehydrated by sublimation using a Polaron LT7400 (Fisons Instruments) and viewed on a cryostage mounted in a Philips XL30 microscope. Scanning probe microscopy (SPM) utilizes a sharp probe moving over the surface of a sample in a raster scan. In this study the probe is a tip on the end of a cantilever which bends in response to the force between the tip and the sample (atomic force microscopy). SPM involves virtually no sample preparation and is done in ambient conditions, so the risk of artifacts is lower than with most types of EM. For SPM of frog glue, moist type I glue was pressed repeatedly against a glass microscope slide or reconstituted glue was smeared onto the glass and allowed to dry. The adhered material was rinsed briefly with water to remove salts and then air-dried. SPM imaging was done in air at room temperature using a Digital Instruments Dimension 3000 instrument equipped with a silicon Pointprobe ($k \approx 60$ N/m) when operated in tapping mode (where the tip is oscillated) and a silicon nitride probe ($k \approx 0.06$ N/m) when operated in contact mode (where the tip is dragged without oscillation).

Statistics. Mean values are reported \pm standard error of the mean. Unless stated otherwise, differences between datasets were tested for significance ($p \leq 0.05$) using an unpaired two-tail P test (Instat).

Results

Glue Collection. Freshly secreted frog exudates had a pH of ~ 6 . Washing the backs of exudate-producing frogs in

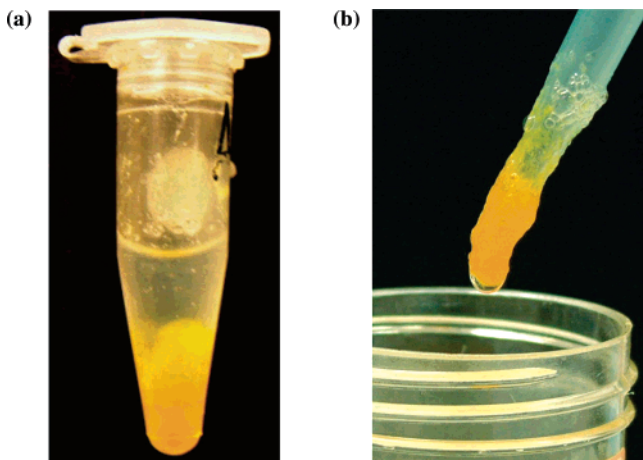


Figure 1. Solid forms of frog glue. (a) Frog exudate was collected in PBS/10 mM Cys·HCl, pH 4.5, and the resulting emulsion was allowed to settle for 3 h at 4 °C. The upper phase is a colorless liquid, while the lower one is a translucent yellow plug of sticky elastic solid (type I glue). (b) Recovery of solid glue from a glue solution. Type I glue was dissolved in 5% (v/v) acetic acid. When concentrated NaCl solution was slowly pipetted into the solution, solid glue could be harvested onto the plastic pipet tip dispensing the salt solution (see text).

PBS/10 mM Cys·HCl, pH 4.5, conveniently emulsified the glue solids which, on settling, consolidated into a cohesive plug. In so doing, the initial creamy yellow suspension resolved into two phases: an upper phase consisting of a colorless and nonviscous liquid fraction and a lower one comprising a sticky and elastic plug of translucent yellow solid (type I glue) (Figure 1a). (To distinguish the set glue from liquid forms and fractions we refer to it as a solid, although strictly speaking it is a hydrogel). In contrast, when the frogs were irrigated using water or 20 mM phosphate buffer, pH 6.2, the glue solids were not emulsified but rather formed aggregates of translucent yellow elastic solid. Glue solidification was seeded by foreign objects and the bulk of the glue material accumulated on the electrode that was being used to stimulate secretion. Under these conditions, the mass of yellow solid on the electrode (type II glue) was bonded avidly to the metal and the solid was much more cohesive (i.e., firmer or more rubber-like) and much less tacky than type I glue. Similar results were obtained when exudate was collected in the absence of any irrigation. Once scraped off the original surface, the solidified neat exudate (type III glue) was strongly cohesive but not very adhesive. To distinguish between the effects of redox state and pH on glue solidification, some other collection conditions were tested. Irrigation of exudate-producing frogs with 50 mM acetic acid or 50 mM ascorbic acid resulted in clear viscous solutions (pH ~2.5) rather than the formation of solid glue. Irrigation of exudate-producing frogs with 20 mM phosphate buffer/10 mM Cys·HCl, pH 6.2, did not emulsify the solids. The glue solidified in the same manner as type II glue, while in terms of physical properties it appeared to be intermediate between type I and type II glue.

Macroscopic Strength Tests. Freshly secreted neat exudate was observed to bond polypropylene disks in an elastic manner with a prompt tensile strength of 57 ± 6 kPa ($n = 8$). Each separated joint showed a mixture of adhesive and

cohesive failure, with one type dominating 50% of the tests while the other dominated the remainder. When separated disks were rejoined and stored humidified for 24 h at 4 °C, they were found to have a tensile strength of 78 ± 8 kPa ($n = 8$). When the joints were again reformed and stored humidified for a further 1 h at 21 °C, they were found to have a tensile strength of 64 ± 5 kPa ($n = 8$). The three sets of tensile strength data were statistically indistinguishable. It is clear that reforming separated joints by hand rapidly restores most of their strength, with more than 80% of the original bond strength returning within 1 h. The elastic modulus was also unaffected by breaking and reforming of the joint; for example, a modulus of 402 ± 56 kPa was obtained during the second test and 394 ± 48 kPa during the third. Illustrative stress–strain plots for exudate-bonded polypropylene disks are shown in Figure 2, with an enlargement of the initial regions (used to calculate modulus) shown in Supporting Information Figure 1a. Pre-solidified frog glue was also able to bond polypropylene but was considerably less effective than freshly secreted exudate. Thus, moist type I frog glue was found to bond polypropylene disks in an elastic manner with a tensile strength of 6.3 ± 0.3 kPa ($n = 8$), weaker than the bond provided by freshly applied UHU Stic (11.7 ± 1.2 kPa) or Blu-Tack (22.5 ± 3.7 kPa). Despite its impressive tackiness toward glass, plastic, metal, and wood, moist type I glue displayed no affinity for deformable hydrophilic surfaces such as solid agar.

Craft stick pairs that had been bonded in lap-joint configuration using moist type I frog glue and then allowed to dry completely displayed a mean shear strength of 1.7 ± 0.3 MPa ($n = 6$). Under these conditions the dried glue showed bond strengths greater than dried UHU Stic (0.9 ± 0.4 MPa) and comparable to set PVA glue (1.3 ± 0.2 MPa) or cured cyanoacrylate glue (1.7 ± 0.7 MPa). Indeed, when type I glue was used to bond a nickel spatula to a hard surface bound with poly(tetrafluoroethylene) (Teflon) tape and allowed to dry, the spatula could not be removed without tearing a hole in the tape.

In strength tests of moist or dry type I glue there seemed to be no difference between glue sourced from different frogs, and glue that had been dissolved and resolidified before use (see below) provided dry bond strengths similar to glue that had not (data not shown).

Nanomechanical Measurements. A nanomechanical force–distance study was conducted on samples of type I and type III glue in water. For each glue type, $n = 8$ throughout. Representative curves for individual experiments are shown in Figure 3; some curves suggested multiple pull-offs, in which case the reported adhesion value was that corresponding to the highest observed (negative) deflection. The measurements indicated that the mean elastic modulus was 171 ± 40 kPa for type I glue and 1034 ± 392 kPa for type III glue. The two forms of glue displayed mean resilience values of $43 \pm 2\%$ and $56 \pm 3\%$, respectively, a difference which, though small, was statistically significant. Mean values for adhesion were difficult to estimate because some samples, especially those of type I glue, proved too sticky. In such cases the retracting tip would draw a strand of glue from the sample, and this would remain unbroken at

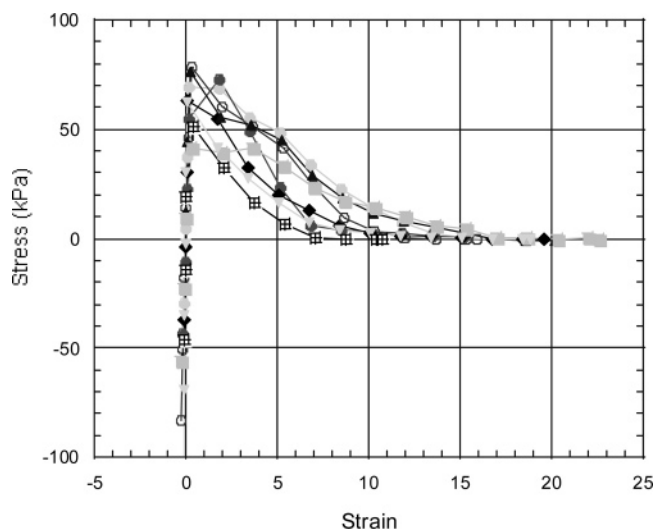


Figure 2. Instron stress–strain plots for polypropylene bonded by neat exudate and stored humidified. Joints under compression at the start of the test were extended to failure and beyond; each of the eight symbols represents the data obtained from one such test. While representative of such joints in general, these particular curves were gathered using joints that had been separated and reformed twice. Note that strain is shown as a dimensionless factor (strain = 1 denotes a doubling in thickness of the glue layer). The initial negative stress values are a consequence of manually maintaining a compressive stress on each joint while fixing it into the testing rig (a precaution taken to ensure the joint was not subjected prematurely to tensile stress during mounting). In magnitude it would not exceed the compression stress applied to form the joint in the first instance, and it did not correlate with the bond strength observed.

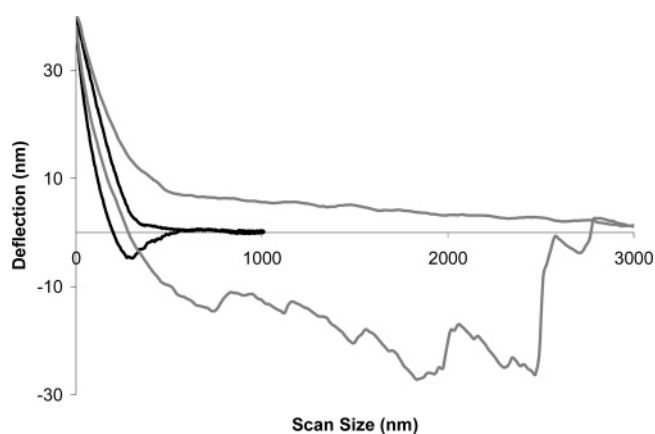


Figure 3. Nanomechanical force–distance curves obtained using a scanning probe microscope. For each glue type, five of the eight curves corresponded to single pull-offs while the remainder were more complex and suggestive of multiple pull-offs. The mean adhesion values for single pull-offs were 3.5 ± 0.6 and 0.7 ± 0.4 nN for type I and type III glue, respectively, while the mean adhesion values for the complex curves were 13.3 ± 4.1 and 3.9 ± 1.7 nN, respectively. The curves shown here are for type I glue and illustrate a single pull-off (black) and a complex curve (grey). For each cycle, the upper trace represents movement of the probe toward and into the sample (penetration) while the lower trace represents the reverse (retraction). Scan size denotes probe travel along the z axis.

full probe retraction (1 cm). In regions where it was low enough to be measured, a mean adhesion value of 7.2 ± 2.3 nN was calculated for type I glue and 1.9 ± 0.9 nN for type III glue. Overall, the nanomechanical results agree with our experiences on the macroscopic level in which the type III solid seems to be denser, more rubbery, and less tacky than the type I material.

Table 1. Amino Acid Composition of Frog Glue Samples (Mol %)

amino acid	residual liquid ^a	type I solid	type II solid	type III solid	solid (mean)
Asx ^b	8.97	6.83	7.26	7.62	7.24
Thr	4.24	4.51	4.36	4.46	4.44
Ser	4.22	3.57	3.96	3.91	3.82
Glx ^b	14.59	13.71	14.42	14.26	14.13
Gly	14.67	14.50	18.36	14.52	15.79
Ala	3.84	2.53	2.86	2.94	2.78
Cys/2	0.86	0.87	0.46	0.80	0.71
Val	4.30	6.61	6.14	5.91	6.22
Met	1.81	0.94	1.13	1.25	1.11
Ile	6.59	4.43	4.62	5.24	4.76
Leu	8.49	6.60	6.80	7.28	6.89
Tyr	2.13	2.20	2.24	2.18	2.21
Phe	5.38	3.48	3.80	4.11	3.79
Lys	6.54	5.58	5.82	5.91	5.77
His	2.49	3.31	3.04	3.02	3.13
Arg	3.16	3.77	4.00	3.60	3.79
Pro	6.82	9.91	8.27	8.18	8.79
Hyp	0.92	6.65	2.44	4.80	4.63
L-Dopa	n.d. ^c	0	0	0	0
Hyl	0	0	0	0	0

^a Liquid fraction remaining above solid type I glue after the latter had settled out from its initial emulsion. ^b Since deamination during acid hydrolysis means that Asn cannot be distinguished from Asp and Gln cannot be distinguished from Glu, the two groups are presented together as Asx and Glx, respectively. ^c n.d. = not determined.

Biochemical Composition. Weighing pellets of type I and type III glue before and after vacuum-drying revealed that fully hydrated glue contained 85–90% (w/w) water, while protein assays indicated that the moist type I glue was ~10% protein (w/w). Dry glue was brittle, but overnight rehydration could return it to a state indistinguishable from the starting material. Despite the very high water content of fully hydrated glue, the material handles more like an elastic solid (e.g., a water-laden sponge) that is inclined to retain its shape than a viscous dilute hydrogel that is prone to deformation and flow. To distinguish the set glue from liquid forms and fractions we refer to it as a solid, although strictly speaking it is a hydrogel.¹⁷ A colorimetric assay for carbohydrate indicated that vacuum-dried type I glue contained only 0.75% (w/w) glucose equivalents. Amino acid analyses were done on different types of frog glue. The results (Table 1) indicated that the solid glue types I–III had similar compositions, being rich in Gly, Pro, and Glx and having a significant 4-hydroxyproline (Hyp) content. 5-Hydroxylysine (Hyl) was not detected, and no L-Dopa was detected even when special hydrolyses were conducted to preserve this residue. The amino acid composition of the liquid fraction remaining above solid type I glue after it had settled out was generally similar to (although much less concentrated than) that of the solid fraction, except that it contained relatively little Hyp (Table 1).

SDS–PAGE of the glue revealed a characteristic pattern of proteins spanning a large size range, with apparent molecular masses ranging from 13 to 400 kDa (Figure 4a). The largest protein, Nb-1R (apparent molecular mass \approx 350–500 kDa), was also the most abundant. Typically this protein ran oddly on gels, giving a wide and irregular band which seemed to comprise a jumble of wavy substructures.

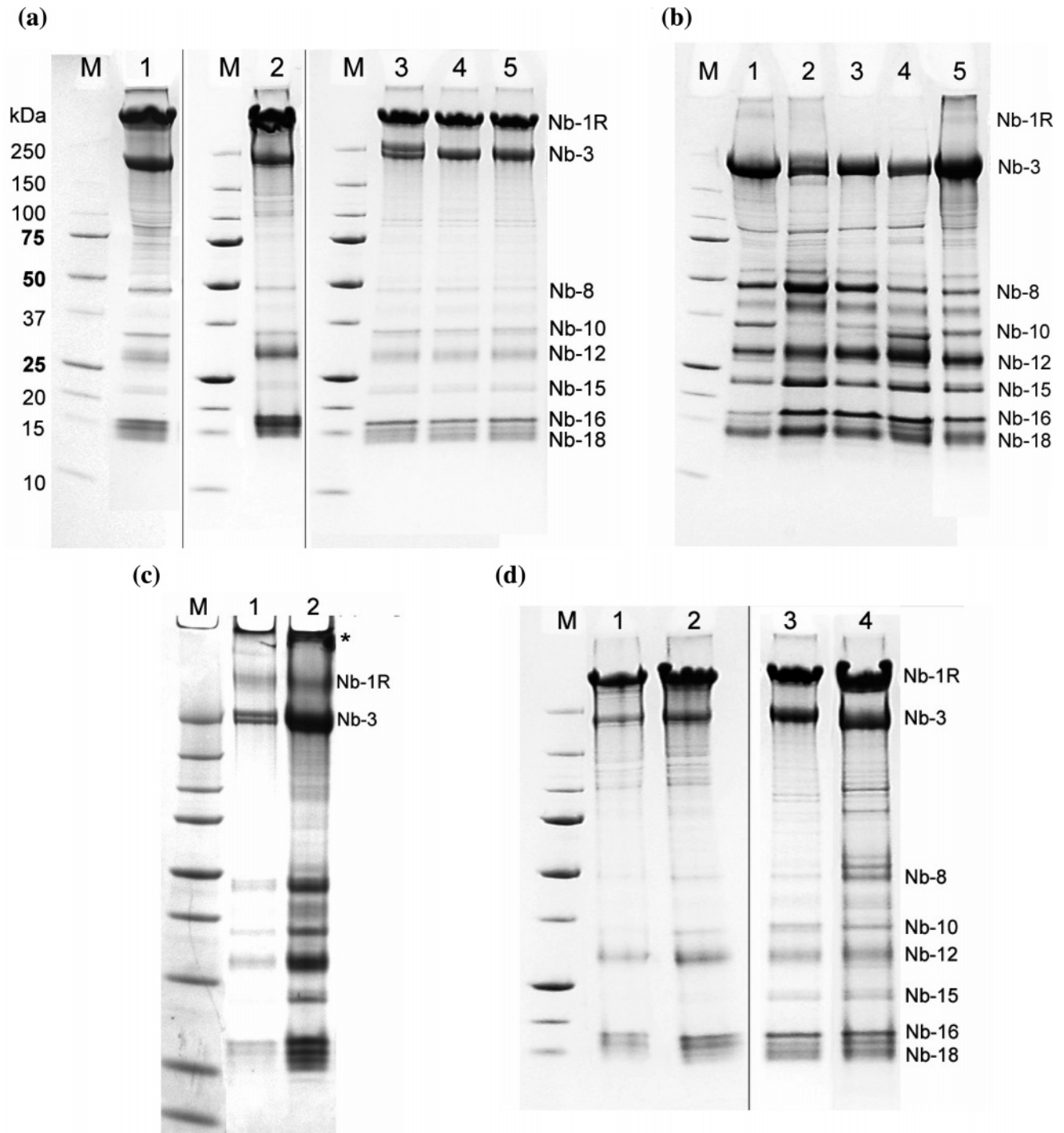


Figure 4. SDS-PAGE of glue samples. Unless otherwise stated, each sample lane within a panel represents material from a different frog. Marker lanes are indicated (M), and the molecular masses of the standard proteins (kDa) are shown at the left of the figure. (a) All types of solid glue gave rise to the same characteristic pattern of proteins, which spans the size range from 13 to ~400 kDa. This panel shows samples of type I glue (lanes 1 and 2) and type II glue (lanes 3–5). Prominent bands have been assigned identifying numbers, which are shown at the right of the figure; Nb derives from *N. bennetti*. Some bands may actually be groups of proteins with similar sizes, and indeed we sometimes observed splitting of bands into discrete components (e.g., compare Nb-3 in lanes 3 and 4). For simplicity we have assigned a single identifying number to species that usually appear as a single band on these gels. The largest species, Nb-1R, is the most abundant, and typically this band has an odd turbulent appearance. (b) The liquid fractions remaining after solidification of type I and type II glue samples contain many of the same glue proteins found in the solid phase, including Nb-3, but in no case was any Nb-1R observed to remain in the liquid fraction. This gel shows samples of liquid from type I or II glue collections (lanes 1–5). (c) If glue samples are not reduced before electrophoresis (lanes 1 and 2) the Nb-1R band is faint and material of high molecular mass (marked with an asterisk (*)) fails to enter the gel. The R in Nb-1R derives from the appearance of this band in SDS-PAGE of reduced (but not in nonreduced) samples. (d) Glue subjected to reconstitution (i.e., dissolution and resolidification) *in vitro* gave essentially the same band pattern as the original solid. This panel shows type I glue before and after reconstitution (lanes 1 and 2, respectively) and type II glue before and after five sequential rounds of reconstitution (lanes 3 and 4, respectively).

In collections of type I or type II glue, a survey of the liquid fractions remaining after glue solidification showed that a proportion of many glue proteins, including the second most

abundant protein Nb-3, was likely to remain in the liquid fraction but that Nb-1R always partitioned completely into the solid fraction (Figure 4b). Nb-1R was also unique in its

ability to form disulfide-mediated multimers. In the absence of reducing agent, most of the Nb-1R content would have a molecular mass that was too large to enter the gel (Figure 4c). Apart from this phenomenon, there was no indication of extensive covalent protein cross-linking in any of the three glue types. Indeed, SDS-PAGE (of samples reduced before loading) detected no differences between the solid glue obtained when exudates were collected in air by washing with 20 mM phosphate buffer, pH 6.2 (i.e., type II glue), and further exposed to air at 22 °C for 30 min before freezing, and that obtained when exudates were collected under argon by washing with 20 mM phosphate buffer/10 mM Cys·HCl, pH 6.2, or with PBS/10 mM Cys·HCl, pH 4.5 (i.e., type I glue), and snap-frozen immediately under argon (Figure 4a, and data not shown). Likewise, the three solids were indistinguishable in terms of amino acid composition (Table 1, and data not shown). This suggests that apart perhaps from the formation of disulfide bonds, the oxidative cross-linking of glue proteins does not constitute a normal part of the glue-setting process.

Gel filtration chromatography of dissolved type I glue was undertaken in an attempt to purify individual proteins. It was unsuccessful because, even in the presence of denaturants, the dissolved glue proteins adsorbed avidly to the chromatography matrix. Columns rapidly became blocked, and harsh treatments were required to rehabilitate them. Only the Superdex-200 column afforded any eluted peaks, and these (not shown) were unexpectedly small, poorly reproducible, and typically appeared after the inclusion volume (V_t). The peaks contained insufficient protein to detect in SDS-PAGE, confirming that most of the protein had bound irreversibly to the column matrix.

Solubilization and Solidification. Type I glue could be fully dissolved in a matter of hours at room temperature in 5% (v/v) acetic acid, 10% (w/v) SDS, 5M guanidinium hydrochloride (pH 5), or 10 mM H_3PO_4 . Interestingly, the pH of unbuffered solvents (such as the SDS solution) rose by several pH units as the glue dissolved. Type I glue was dissolved less effectively by 4.7 M urea, pH 5, and even less so by 10–100 mM H_2SO_4 or 0.05% (v/v) acetic acid. Type I glue could also be dissolved by overnight incubation in 9 M LiBr at 37 °C. The solubility of other glue types was not explored extensively, but as far as tested, they behaved much like type I glue. For routine purposes samples of all types of solid glue were dissolved in 5% (v/v) acetic acid, which permitted concentrations of up to 10 mg of protein/mL of solution. Although 0.05% (v/v) acetic acid was not effective at dissolving solid glue, concentrated solutions could be achieved by dissolving the solid in 5% (v/v) acetic acid and then dialyzing the solution against 0.05% (v/v) acetic acid at 4 °C. Rheological tests done on type I glue dissolved in 0.05% (v/v) acetic acid revealed that the solution was shear thinning. At a steady shear rate of $0.1\ s^{-1}$, the viscosity was $\sim 10\ Pa\cdot s$, whereas at $1000\ s^{-1}$ it had dropped below $0.01\ Pa\cdot s$ (Supporting Information, Figure 1b).

Raising the ionic strength of glue solutions caused the glue components to self-assemble spontaneously into a tacky and elastic solid which retained most of the functionality of the original (i.e., undissolved) glue. Thus, if a small volume of

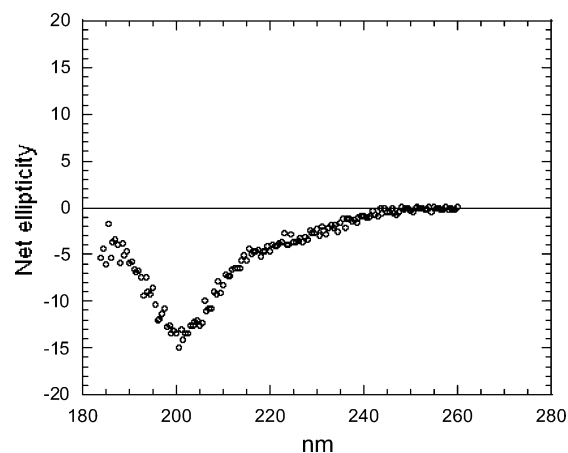


Figure 5. Circular dichroism (CD) spectrum of type I glue. The spectrum indicates a relatively unstructured system dominated by random coil and/or containing nonstandard elements.

5 M NaCl solution was gradually dispensed to a final concentration of 0.8–1.0M NaCl into a type I glue solution of ≥ 4 mg of protein/mL in 5% or 0.05% (v/v) acetic acid, then solid glue materialized as fibrils or particles that that could be grown or harvested as a translucent yellow sticky solid on the outside of the pipet tip dispensing the salt solution (Figure 1b). Invariably some material was not recovered by this process, and the remaining liquid often had a turbid white appearance. Type II glue was equally amenable to reconstitution *in vitro*, and likewise solid glue could also be recovered by adding 5 M NaCl to the viscous liquid obtained from exudate-producing frogs that had been irrigated with 50 mM acetic acid. Experiments in which type I glue was reconstituted *in vitro* showed that the solid was able to form in highly denaturing solutions (e.g., acid solutions containing 4.7 M urea or 5 M guanidinium hydrochloride) and that its formation was completely unaffected by high concentrations of reducing agents (e.g., 1% (v/v) 2-mercaptoethanol). Removing trapped acetic acid and salt from reconstituted type I glue by soaking it in water increased the translucence and adhesiveness of the solid, although it still seemed to remain softer and less tacky or elastic than unreconstituted glue. The reconstituted material could be subjected to many further rounds of dissolution and resolidification without any noticeable change in its physical properties. Indeed, SDS-PAGE revealed that type I glue which had undergone five rounds of serial reconstitution still contained all of the proteins present in the original material (Figure 4d). In addition to raising the ionic strength we noted other ways in which glue could be solidified from clear solutions *in vitro*. These treatments, which were not investigated extensively, included the addition of dehydrating agents such as poly(ethylene oxide) and dialysis against pure water or poly(ethylene oxide) solutions.

Some apparent similarities between frog glue and mammalian elastin (see below) prompted us to look for others. We discovered that, like frog glue, soluble bovine elastin could be recovered from solutions as a sticky solid simply by adding concentrated NaCl solution. On the other hand, we found that solutions of the frog glue would not undergo an elastin-like phase separation (coacervation) upon heating. Solutions of type I glue remained clear at various temper-

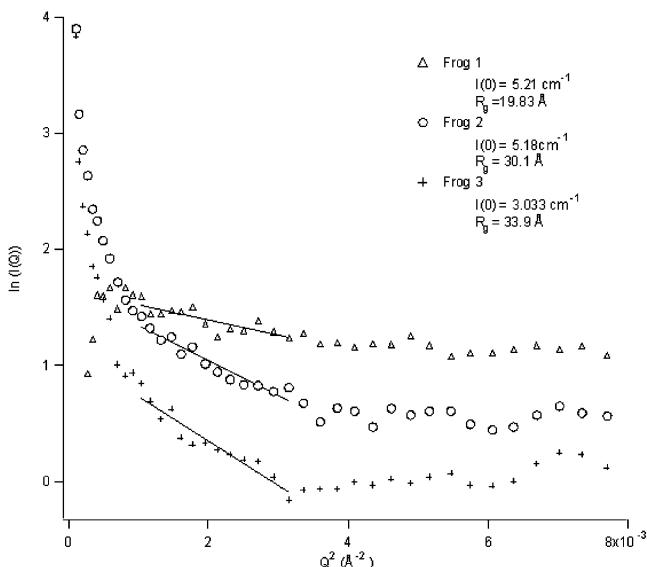


Figure 6. Small-angle X-ray scattering (SAXS) data for type I glue. Scattering intensities are plotted as $\ln I(q)$ against q^2 , where $I(q)$ is the radially averaged background-corrected scattering intensity (cm^{-1}) and q is the scattering vector (\AA^{-1}). Plots and model-independent Guinier analyses for three forms of glue: dissolved glue (Frog 1, Δ), moist solid (Frog 2, \circ), and dry solid (Frog 3, $+$). The fits indicate $R_g = 2.0 \pm 0.2$, 3.0 ± 0.2 , and 3.4 ± 0.2 nm, respectively.

atures up to 99°C and when refrigerated thereafter. Interestingly, heating solutions of glue to 80°C or more prevented the subsequent recovery of functional glue by addition of concentrated NaCl solution, which now precipitated particles that were neither adhesive nor cohesive.

Spectroscopy. Magic angle spinning ^{13}C NMR of dried type I glue only detected protein (Supporting Information, Figure 2a). Even when cross-polarization was used to reduce the signal from the polypeptide backbone, only standard amino acid side-chain signals were observed (Supporting Information, Figure 2b). D_2O extracts of type I glue also gave a ^1H NMR spectrum typical of protein, along with some small nonstandard signals (δ 7.5–8.5 ppm) (Supporting Information, Figure 2c). The absorbance spectrum of dissolved frog glue (not shown) had a maximum at 462 nm and pronounced shoulders 26 nm either side of the main peak, a pattern characteristic of carotenoid chromophores.¹⁸ The CD spectrum of dissolved type I glue (Figure 5)

indicated a poorly structured system dominated by random coil and/or containing nonstandard elements. Deconvolution suggested the presence of no α helix, 36% β -elements, and 64% random coil.

Scattering Studies. SANS and SAXS studies gave curved plots of $\ln I(q)$ against q^2 , suggesting that aggregates were present, so the lowest value for the radius of gyration (R_g) was extracted from each curve to provide a mean value for the particle population that was scattering most strongly. A SANS study on dissolved type I glue (Supporting Information, Figure 3a) indicated $R_g = 3.6 \pm 0.2$ nm, consistent with a compact protein of ~ 170 kDa. SAXS studies (Figure 6) undertaken on three forms of type I glue—dissolved, moist solid, and dry solid—indicated $R_g = 2.0 \pm 0.2$, 3.0 ± 0.2 , and 3.4 ± 0.2 nm, respectively, consistent with compact proteins of ~ 30 , ~ 85 , and ~ 135 kDa, respectively. The SANS and SAXS results for dissolved glue ($R_g \approx 3.6$ and 2.0 nm, respectively) are in good agreement for initial experiments and might be reconciled further by more detailed studies. The results to date suggest that both techniques are observing glue protein monomers. One possible explanation for the discrepancy between the molecular masses inferred (assuming globularity) from the R_g values (30–170 kDa) and those observed by SDS–PAGE (where most of the mass appears to reside in a 300–500 kDa species) is that the scattering particles are in fact elongated. More sophisticated studies (e.g., synchrotron SAXS and SANS with deuterated solvents) would provide more reliable information about particle shape. DLS studies of dilute solutions of type I glue (Supporting Information, Figure 3b) were used to determine the size distribution by volume (Figure 7). Scattering was dominated by populations of large particles with mean hydrodynamic radii $R_h = 150$ –1000 nm, which must correspond to very large assemblies of glue proteins. Populations of small particles ($R_h = 2$ –10 nm) were often but not always seen. When detected, they accounted for a total volume comparable to that of the large-particle populations. Since the small particles had R_h values comparable to the R_g values seen by SANS and SAXS, it is likely that these populations are real but difficult to detect by DLS in the presence of larger particles. Their R_h values are consistent with compact proteins of 30–900 kDa, so many of these

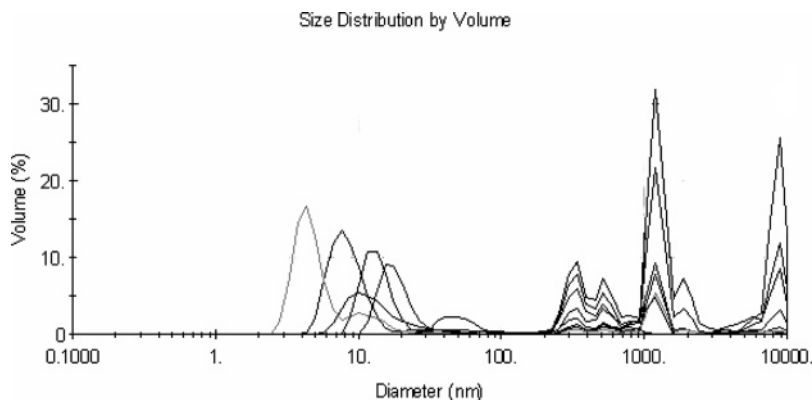


Figure 7. Dynamic light scattering (DLS) by dissolved type I glue presented in terms of size distribution by volume. Eight distributions are shown; each one represents 12 measurements of 10 s and shows the percentage of the total particle volume as a function of hydrodynamic diameter ($2R_h$). A particle population of $2R_h = 500$ –2000 nm is always seen; another of $2R_h = 4$ –20 nm is often seen, while yet another of $2R_h = 5000$ –9000 nm is sometimes seen.

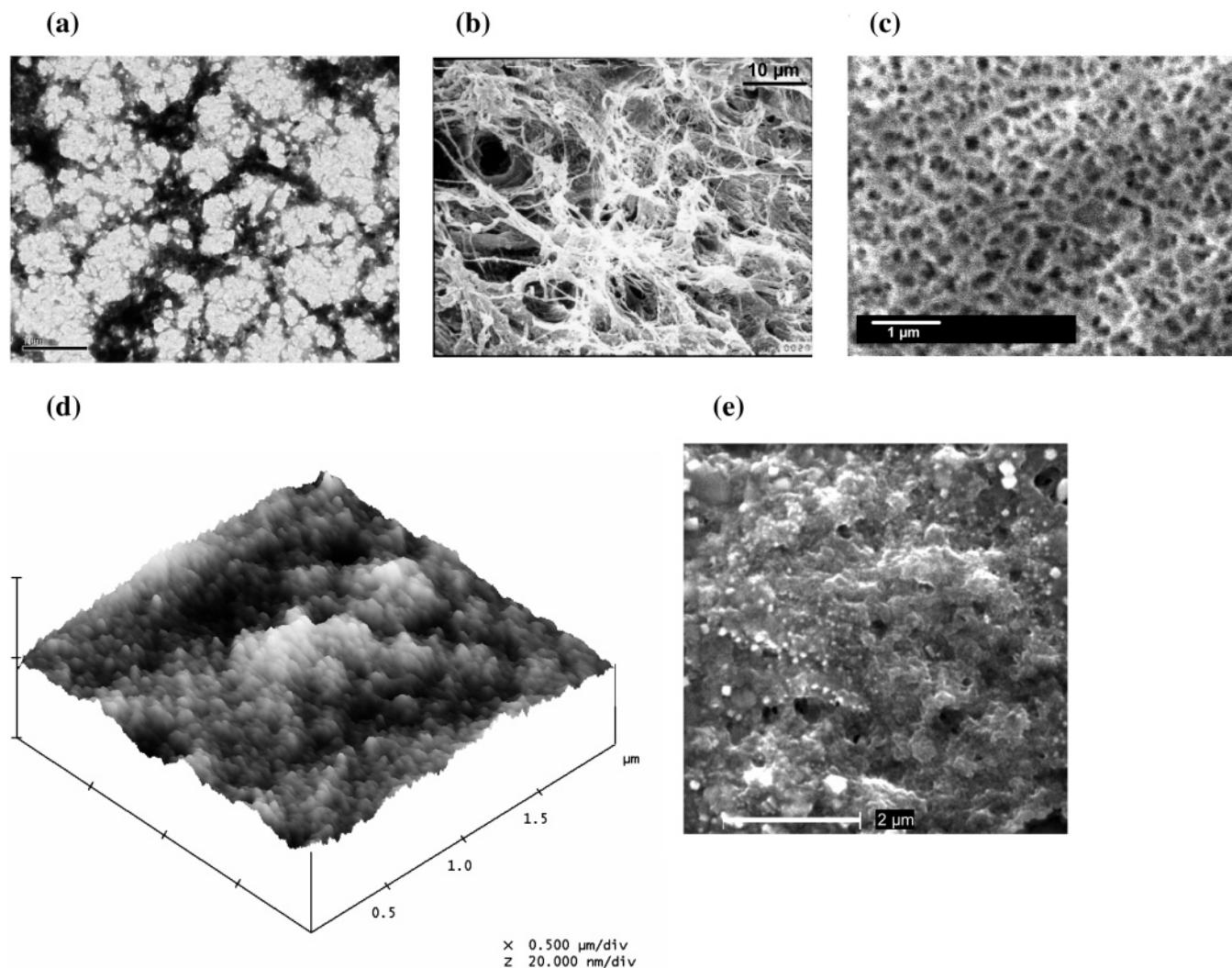


Figure 8. Images showing interior (a–c) and surface (d, e) regions of reconstituted (a, e) or unreconstituted (b–d) type I glue samples. Reconstitution (i.e., dissolution and resolidification *in vitro*) is explained in the text. (a) TEM. (b) SEM, low magnification. (c) CryoSEM. (d) SPM, 3D height image taken in contact mode. (e) SEM, high magnification; the embedded white cubes are crystals of salt remaining from the reconstitution step.

small particles are likely to be glue protein monomers. In some but not all experiments a third population containing very large aggregates was also seen ($R_h = 2500\text{--}4500\text{ nm}$). Dissolved type I glue particles gave a narrow microelectrophoretic peak with a zeta potential of $+29\text{ mV}$ (Supporting Information, Figure 3c). The high positive charge was unsurprising in view of the acidic environment (pH 2.4).

Imaging. TEM of exudates diluted with various acidic and/or reducing solutions revealed micelle-like particles of $25\text{--}50\text{ nm}$ radius aligned in chains, large globules of $300\text{--}400\text{ nm}$ radius, and bundled filaments (Supporting Information, Figure 4a–d). However, electron micrographs of solid glue gave quite different results. TEM of reconstituted type I glue revealed a honeycomb pattern (Figure 8a) in which the pores (typically $75\text{--}175\text{ nm}$ in radius) were defined by interlocking knobby struts or sheets (typically $10\text{--}20\text{ nm}$ wide). No substructures were seen within the latter even at high magnification (Supporting Information, Figure 4e). Low-magnification SEM images of unreconstituted glue supported the TEM results, revealing an open meshwork of fibers (Figure 8b). CryoSEM of freeze-fracture surfaces from unreconstituted type I glue showed a range of pore sizes,

but individual micrographs were usually comprised exclusively of either very large pores ($0.5\text{--}1.5\text{ }\mu\text{m}$ radius, not shown) or very small pores ($50\text{--}150\text{ nm}$ radius; Figure 8c). CryoSEM images of reconstituted type I glue were mainly of the latter type (data not shown). SPM images of unreconstituted type I glue deposits (Figure 8d) suggested that the glue consisted of spherical particles about $10\text{--}50\text{ nm}$ radius and revealed patches with some large pits ($\sim 230\text{ nm}$ radius) where some larger globules ($\sim 100\text{ nm}$ radius) occurred on top of a bed of smaller ones (not shown). In general, the SPM surface of reconstituted glue was similar to that of unreconstituted glue. High-magnification SEM of a reconstituted type I glue surface (Figure 8e) revealed a knobby microstructure permeated by pits and pores/channels ($20\text{--}150\text{ nm}$ diameter) whose topography was similar to the surface imaged by SPM.

Discussion

Material Properties of the Glue. To distinguish the set frog glue from liquid forms and fractions we refer to it as a solid, although strictly speaking it is a hydrogel.¹⁷ The moist

solid functions as a pressure-sensitive adhesive whose bond strength is largely unaffected by breaking and reforming of the joint. Like other pressure-sensitive adhesives,¹⁹ the frog glue is most effective at bonding rigid surfaces which can be placed under pressure. In tests comparable to ours (i.e., using sanded polypropylene disks) other researchers determined tensile strengths of ~ 100 kPa for freshly secreted Tomato Frog exudate and 20–63 kPa for freshly secreted glues from other frogs and salamanders.¹ Thus, with a tensile strength of 57–78 kPa, freshly secreted *N. bennetti* exudate sets with a bond strength comparable to those for adhesive secretions from other amphibia. The *N. bennetti* values are intermediate between the tensile strengths reported for the adhesion of marine mussel plaque to hydrophobic substrates (~ 13 kPa) and to hydrophilic ones (320–860 kPa).²⁰ In its hydrated form, the frog glue that we studied has a tensile strength lower than that of the cement adhering adult barnacles to rigid substrata (150–490 kPa)²⁰ or that of the mucus used by limpets for attachment (230–518 kPa)²¹ but is within the range reported for holothurian Cuvierian tubules adhered to glass (30–135 kPa).²² By way of further comparison, the synthetic pressure-sensitive adhesives in clinical use for drug delivery typically have tensile strength values of ~ 16 MPa for hydrophobic polymers (DuroTak, 34–4230, etc.) and ~ 10 kPa for hydrophilic ones (Carbopol, Noveon, etc.).²³

The nanomechanical force–distance curves for the frog glue (Figure 3) are qualitatively similar to the single and multiple pull-offs observed when the same technique was applied to the hydrated glycoprotein adhesive used by spores of the green alga *Ulva linza* (formerly *Enteromorpha linza*).²⁴ When the adhesive forces exhibited by type I frog glue (in freshwater) were low enough to be measured, the mean adhesive force was ~ 7.2 nN, with a top individual value of 18.9 nN, whereas the corresponding mean value for algal spore glue (in seawater) was ~ 17 nN, with a top individual value of 46 nN.²⁴ The values for the algal spore glue were greater than those obtained when the same technique was applied to other biological bonding agents,²⁴ so we may conclude that the frog glue is relatively effective. The same SPM study found that the mean (compressive) elastic modulus of freshly secreted algal spore glue was ~ 540 kPa, a value midway between the corresponding modulus values we observed for type I glue (~ 170 kPa) and type III glue (~ 1000 kPa), but observed that this increased rapidly to a mean value of ~ 5 MPa as the algal glue cured.²⁴

As might be expected, the elastic modulus determined nanomechanically for type III frog glue under compression in water (~ 1000 kPa) was comparable to that for an equivalent form of the glue (i.e., freshly set undiluted exudate that was still moist) tested macroscopically under tension in air (~ 400 kPa). These values are near or above the high end of the range for the conventional synthetic pressure-sensitive adhesives used in drug delivery, which typically have elastic modulus values of 100–500 kPa for the hydrophobic polymers and 9–90 kPa for the hydrophilic ones.²³ Frog glue (types I and III) exhibited 43–56% resilience in water, substantially lower than the values of $\sim 90\%$ published for elastin, collagen, and resilin tested in

aqueous environments.²⁵ As one might expect,¹⁷ dry joints involving rigid substrates were no longer elastic but provided the highest bond strengths. The shear strength values for wooden joints bonded by dried *N. bennetti* glue (~ 1.7 MPa) are comparable to those reported for similar joints bonded by glue from the related frog *N. melanoscaphus* (~ 2.8 MPa)² and match those reported for epoxy glass substrates bonded by dried Montana C-902 Polymer, a bacterial exopolysaccharide now sold as a commodity adhesive.²⁶

The frog glue binds most avidly to the surface on which it first solidifies. It is likely that the adhesive determinants in the newly secreted material seek interaction partners and, in the absence of a suitable adherend (either at the time of secretion or subsequently when scraped off the original surface), they simply interact with each other and/or the buffer components, resulting in a solid that is still sticky but not nearly as adhesive as the nascent exudate. The glue is soluble in dilute acids, which may in part explain why type I glue (pH ~ 4.5) is softer and more tacky than type II or III glues (pH ~ 6). Glue reconstituted (i.e., dissolved and then resolidified) in vitro retained much of the functionality of the original solid but lacked the bonding power of freshly secreted exudate. Our inability to recover the full adhesive power of freshly secreted exudate during reconstitution may reflect a number of factors, including unnatural solvation or denaturation of glue proteins by the acetic acid, dilution or loss of nonprotein components during reconstitution, or a reliance in the natural process upon biophysical subtleties that we are unable to mimic in vitro. On the last point, it seems likely that the physicochemical processes governing the initial solidification of fresh exudate (which occurs spontaneously from a creamy emulsion at pH ~ 5) would differ from those controlling the resolidification of dissolved glue (in which salt is added gradually to clear solutions at pH ~ 2).

Composition, Mechanism, and Structure of the Glue.

A biochemical assay indicated that dry glue has a very low carbohydrate content ($< 1\%$ (w/w) glucose equivalents), and this was supported by NMR spectroscopic analyses, which detected little apart from protein. The observed sugar content would be consistent with conventional *N*- or *O*-linked glycosylation of some of the glue proteins. Amino acid analysis showed that the solid frog glue contains substantially more Gly, Pro, and Glx than the average vertebrate protein²⁷ but has an unexpectedly low content of Ala, Ser, and Met. Many structural proteins are rich in Gly and Pro, although the levels of Gly in the frog glue are only around one-half those found in collagen and elastin. Elastomeric proteins can be sorted into discrete groups including those rich in Gly, those rich in Gly and Pro, and those rich in Gly, Pro, and Gln.²⁸ The frog glue may be a member of the second group (which contains elastin and spider flagelliform silk) or, if the high Glx level is the result of an elevated Gln content, the third group (which contains spider dragline silk and plant HMW glutenins). It is particularly interesting to note the presence of Hyp in the frog glue at 2.4–6.7 mol %. This range of values, which may reflect different levels of Pro modification by individual frogs, is intermediate between the levels of Hyp observed in elastin (1.0–2.5 mol %) and the

major form of collagen (10 mol %).²⁹ Hyp is also found at high levels (sometimes approaching 20 mol %) in the proteins that comprise the adhesive plaque of marine mussels,^{30–33} but these plaque proteins are also very rich in L-Dopa (up to 30 mol %), a residue that was not detected in the frog glue. On the basis of composition alone, it is not easy to say which well-known biomaterial the frog glue resembles most. For example, the frog glue is similar to elastin in that both are rich in Gly and Pro and both contain some Hyp but no Hyl, but on the other hand the glue is not enriched in nonpolar aliphatic residues and there is no suggestion that it contains Lys cross-links. Edman degradation of glue proteins electroblotted from gel bands yielded a different N-terminal sequence for each of the major proteins Nb-1R and Nb-3, but homology searches with these short sequences did not reveal any meaningful relationships with existing database entries.³⁴ The comparison of frog glue with other biomaterials is continued below in a separate section.

The solidification of the frog glue appears to involve spontaneous and noncovalent assembly of the component proteins. As the largest and most abundant protein in the glue, Nb-1R is likely to be the key structural component, and its complete partitioning into the solid phase during the setting of exudate emulsions suggests that Nb-1R provides the scaffold to which the other proteins attach. Hyp also partitions preferentially into the solid phase (Table 1), suggesting that much of it may be associated with Nb-1R. Moreover, the unusual rippled appearance of the Nb-1R band in SDS-PAGE may result from Nb-1R molecules engaging in adhesive interactions with the polyacrylamide matrix or the plastic gel plates during electrophoresis. Since the high Gly and Pro content of the frog glue allow for an amphipathic protein with regions of substantial hydrophobicity, and since a functional form of solid glue can be reconstituted *in vitro* simply by raising the ionic strength of a glue solution, it seems likely that the self-assembly process relies upon hydrophobic protein-protein interactions.

Disulfide bonds can form between Nb-1R molecules, but since reducing agents did not prevent glue solidification (either *de novo* or during reconstitution *in vitro*), these bonds cannot be an essential part of the setting mechanism. Apart from the ability of Nb-1R to form disulfide-linked multimers, amino acid analysis and SDS-PAGE provided no other evidence of extensive covalent cross-linking in set glue. Specifically, there was no difference in amino acid composition or gel band pattern between type I glue that had been collected and maintained in a highly reducing nonphysiological environment and type II glue that had been given an extended opportunity to undergo enzymatic or atmospheric oxidation at the time of collection. Thus, while most of our glue collections were performed under an inert atmosphere, this precaution appeared to be unnecessary. In a nonreducing environment it is likely that Nb-1R does form intermolecular disulfide bonds within solid glue, and these may enhance its cohesive properties. The firmer and more rubbery nature of types II and III glue relative to type I glue may in part be due to the formation of such bonds. The yellow color of the frog glue appears to be caused by the presence of carotenoids. Since carotenoid chromophores are known to contribute to

Table 2. Microstructural Data Obtained from Scattering Studies and Microscopy Images

technique and sample ^a	particle radius (nm) ^b	cavity radius (nm) ^b
SANS, dissolved	3.6	
SAXS, dissolved	2.0	
SAXS, moist and air-dried solid	3.0–3.4	
DLS, dissolved	2–10	
	150–1000	
	2500–4500	
SPM, air-dried solid	10–50	230
	100	
SPM, air-dried reconstituted solid	25–50	
	50–150	
TEM, vacuum-dried exudates	25–50	
	300–400	
TEM, vacuum-dried reconstituted solid		75–175
SEM, vacuum-dried solid, low magnification		185–5500
SEM, vacuum-dried reconstituted solid, high magnification	10–100	20–150
CryoSEM, freeze-fractured vacuum-dried solid		50–150
		500–1500
CryoSEM, freeze-fractured vacuum-dried reconstituted solid		50–125

^a Air-dried refers to samples allowed to dry at room temperature, while vacuum-dried denotes desiccation or sublimation under vacuum. Reconstituted glue means glue that was dissolved and resolidified *in vitro* (see text). ^b Numerical values denote approximate means or estimates of range; particle radii calculated from scattering data are R_g or R_h values (defined in the Experimental Section).

dermal pigmentation in amphibia,³⁵ it is perhaps unsurprising to find such compounds in a colored amphibian skin secretion. We have seen no indication that the pigments contribute to the adhesive or elastic properties of the frog glue material.

Although reconstituted glue samples often seemed less adhesive or cohesive than unreconstituted ones, for the most part they yielded similar EM and SPM images and in this section they will be treated jointly. The dimensions of the particles and cavities observed by a variety of scattering and microscopy techniques are summarized in Table 2. In broad terms, scattering studies of dissolved or solid glue and microscopy of glue surfaces revealed particle populations whose mean radii ranged from low nanometer values (probably protein monomers) to aggregates with low micrometer radii; in dry glue the particle radius was often 10–150 nm. In contrast, micrographs of sections or fracture planes from solid glue revealed a lattice of cavities; typically their radii were 50–150 nm, but up to low micrometer values were observed. In at least some cases these cavities probably correspond to the interiors of the spherical structures seen by surface imaging techniques. The spongelike network of pores and channels within the glue certainly explains how the moist solid can accommodate a water content of 85–90% (w/w). We were somewhat surprised to find that DLS did not observe many particles of radius 10–100 nm in glue solutions, since spherical structures in this size range were common in TEM images of exudates and dominated the SPM images of glue surfaces.

Similarities with other Biomaterials. The solubility of frog glue appears to be greater than that of marine mussel

plaque^{30–32} and much greater than that of barnacle cement.^{30,36,37} The abundant protein Nb-1R is unusually large (apparent molecular mass 350–500 kDa) in relation to the dominant proteins in biological adhesives from other organisms, where (in monomeric form) the largest major polypeptides are typically ~100 kDa and only occasionally exceed ~200 kDa.³⁸ For example, the largest of the *Mytilus edulis* (mussel) foot proteins is 110 kDa,^{32,33} the largest major *Megabalanus rosa* (barnacle) cement protein is 100 kDa,³⁷ the *Ulva compressa* spore glycoprotein (a relative of the one whose nanomechanical properties are discussed above) is ~110 kDa,³⁹ the largest protein in the carbohydrate-rich mucus of *Littorina irrorata* (periwinkle) is 65 kDa,⁴⁰ and the largest *Gasterosteus aculeatus* (stickleback) spiggin glycoprotein is 130 kDa. Larger polypeptides are found in the mucus of *Lottia limatula* (limpet) and in the adhesive from the Cuvierian tubules of *Holothuria forskali* (sea cucumbers), whose organic fractions contain 15% and 40% (w/w) carbohydrate, respectively, and whose proteins range in size between 20 and 220 kDa.^{21,41} Many of the proteins found in biological adhesives such as these are rich in Gly and Pro and contain posttranslational modifications such as glycosylations and hydroxylations.³⁸ The high content of Gly and Pro in the frog glue, and the presence of Hyp in both it and the adhesive plaque of *M. edulis*,^{30–33} have already been commented on above. Thus, while Nb-1R seems unusually large relative to the proteins in many other biological adhesives, in other respects the composition of the frog glue is in keeping with what is found in such systems.

Interestingly, the frog glue surfaces imaged by SPM and SEM bear a strong resemblance to the globular/micellar surfaces observed when silkworm silk fibroin samples were imaged by the same techniques.⁴² Moreover, the dissolution of the glue by LiBr solutions and its solidification by poly(ethylene oxide) is strongly reminiscent of the behavior of silk fibroins.⁴² Silkworm fibroin heavy chains are Gly-rich hydrophobic β -rich proteins of ~350 kDa.^{42,43} As such they have several features in common with Nb-1R, a protein of 350–500 kDa that is the main component in a Gly-rich and somewhat hydrophobic mix of glue proteins whose structured regions consist mainly of β -elements. Silk formation is driven by self-assembly but involves complex biophysical processes that are only now being elucidated.^{42,44,45} Equally sophisticated processes may underlie the formation and function of the frog glue; it is certainly tempting to relate the small spheres, large globules, and bundled chains seen in TEM images of frog exudates to the micelles, globules, and fibers involved in silk formation.⁴² The frog glue has compositional similarities not only with silks but also with collagen and elastin, as mentioned above. Moreover, the CD spectrum for dissolved frog glue is almost identical to that of soluble elastin,⁴⁶ and both are sufficiently hydrophobic (or at least amphipathic) that they condense from solution to form a sticky solid when the ionic strength is raised. The elastic modulus of type III glue (i.e., set undiluted exudate) in water was ~1 MPa, very similar to that for bovine elastin in water (1.1 MPa).²⁵ Unlike elastin, though, dissolved frog glue does not coacervate at elevated temperatures. Rather, thermal denaturation seems to cause irreversible damage to the

structure of one or more of the glue components and prevents the recovery of a solid that has glue-like properties.

Thus, while the frog glue is also likely to resemble other biomaterials, the most obvious compositional, structural, and functional relationships we could identify at this stage were partial similarities with other biological adhesives and with structural proteins such as silks and elastin. Helical secondary structure elements called β -turn spirals are thought to act as “nanosprings” and are believed to provide high elasticity in a variety of protein biomaterials, including elastin,⁴⁷ silks, and plant HMW glutenins.^{28,48} Given the prevalence of β -elements indicated by the CD spectrum for dissolved frog glue, it is tempting to speculate that β -turn spirals may also underpin the elasticity of the glue. In addition, it makes sense that elastin, which is highly cross-linked via linear and higher-order covalent Lys adducts, fails in strength tests at strain = 1.5²⁵ whereas frog glue, which lacks equivalent cross-links, is highly extensible and fails completely only at strain > 7 (Figure 2). The glue may also have aspects in common with other β -element systems, such as the hydrogels formed by the self-assembly of amphipathic peptides into β -sheet structures,⁴⁹ as with dissolved frog glue, some of these systems gel on addition of monovalent salts.⁵⁰ Considerable further work, including gene cloning and sequencing, is required to establish a detailed mechanism for the frog glue and clarify its relationship with known protein biomaterials.

Applications. Current surgical glues and sealants are either protein-based, in which case they exhibit low bond strength, or synthetic, in which case they form rigid and impervious barriers that hinder wound healing. Our results show that the exudate from *N. bennetti* frogs rapidly and spontaneously forms a proteinaceous pressure-sensitive adhesive that functions well in wet environments. The hydrated solid is highly elastic and consists of a porous mesh that in clinical contexts should allow the diffusion of gases and nutrients. Since some of the cavity radii reported in Table 2 equate to pores with diameters in excess of 10 μ m, it is likely that the hydrated material will also permit a degree of cellular infiltration. Initial experiments suggest that the glue is highly biocompatible,^{2,51} and it has been used successfully to bond severed cartilage tissue both *ex vivo*³ and *in vivo*.^{2,51} In an attempt to develop a commercial product from the natural material, we intend to clone and sequence the genes encoding the major glue proteins and investigate whether recombinant Nb-1R and its component domains possess adhesive and/or elastic properties.

Acknowledgment. We thank Raju Adhikari, Chris Barton, Nick Bartone, Barbara Bojarski, Iko Burgar, Tony Cripps, Mark Greaves, Lawry McCarthy, Roger Mulder, Sarah Taylor, Helmut Thissen, Bert Van Donkallar, Russell Varley, and Jacinta White (CSIRO), Joel Mackay (Sydney University), and Bryn McDonagh (ATA Scientific, Sydney).

Supporting Information Available. Four additional figures (Figure 1: Material properties of solid and dissolved frog glue; Figure 2: NMR spectra of type I glue; Figure 3: Neutron and light scattering data for dissolved type I glue; Figure 4: Additional TEM images of samples of frog exudate

and glue). This material is available free of charge via the Internet at <http://pubs.acs.org>.

References and Notes

- (1) Evans, C. M.; Brodie, E. D. *J. Herpetol.* **1994**, *28*, 502–504
- (2) Tyler, M. J.; Ramshaw, J. A. M. International Patent WO02/22756, 2002.
- (3) Szomor, Z. L.; Appleyard, R.; Tyler, M. J.; Murrell, G. A. C. Pre-Olympic Congress on Sports Medicine and Physical Education and International Congress on Sport Science 7–13 Sep 2000, Brisbane. Online at <http://www.ausport.gov.au/fulltext/2000/preoly/abs297.htm> (accessed Nov 2004).
- (4) MedMarket Diligence Report #S120, Worldwide Wound Sealant Market, 2002.
- (5) Tyler, M. J.; Stone, D. J.; Bowie, J. H. *J. Pharmacol. Toxicol. Methods* **1992**, *28*, 199–200.
- (6) Dubois, M.; Gilles, K. A.; Hamilton, J. K.; Rebers, P. A.; Smith, F. *Anal. Chem.* **1956**, *28*, 350–356.
- (7) Moore, S.; Stein, W. H. *Methods Enzymol.* **1963**, *6*, 819–831.
- (8) Gieseg, S. P.; Simpson, J. A.; Charlton, T. S.; Duncan, M. W.; Dean, R. T. *Biochemistry* **1993**, *32*, 4780–4786.
- (9) Online at <http://www2.umdj.edu/cdrwjweb/> (accessed Nov 2002).
- (10) Aldissi, M.; Henderson, S.; White, J. W.; Zemb, T. *Mater. Sci. Forum* **1988**, *27/28*, 437.
- (11) De la Torre, J. G.; Huertas, M. L.; Carrasco, B. *Biophys. J.* **2000**, *78*, 719–730.
- (12) Svergun, D. I.; Richard, S.; Koch, M. H.; Sayers, Z.; Kuprin, S.; Zaccai, G. *Proc. Natl. Acad. Sci. U.S.A.* **1998**, *95*, 2267–2272.
- (13) Arrio-Dupont, M.; Foucault, G.; Vacher, M.; Devaux, P. F.; Cribier, S. *Biophys. J.* **2000**, *78*, 901–907.
- (14) Duden, R.; Griffiths, G.; Frank, R.; Argos, P.; Kreis, T. E. *Cell* **1991**, *64*, 649–665.
- (15) List, B. M.; Klösch, B.; Völker, C.; Gorren, A. C. F.; Sessa, W. C.; Werner, E. R.; Kukovetz, W. R.; Schmidt, K.; Mayer, B. *Biochem. J.* **1997**, *323*, 159–165.
- (16) Jermutus, L.; Kolly, R.; Foldes-Papp, Z.; Hanes, J.; Rigler, R.; Pluckthun, A. *Eur. Biophys. J.* **2002**, *31*, 179–184.
- (17) Smith, A. M. *Integr. Comp. Biol.* **2002**, *42*, 1164–1171.
- (18) Schmidt-Dannert, C.; Umeno, D.; Arnold, F. H. *Nat. Biotechnol.* **2000**, *18*, 750–753.
- (19) Zosel, A. Cover story: Molecular structure, mechanical behavior and adhesion performance of pressure-sensitive adhesives, 27 Sep 2000. Online at <http://www.adhesivesmag.com/CDA/ArticleInformation/coverstory/BNPCoverStoryItem/0,2103,11474,00.html> (accessed Jan 2005).
- (20) Crisp, D. J.; Walker, G.; Young, G. A.; Yule, A. B. *J. Colloid Interface Sci.* **1985**, *104*, 40–50.
- (21) Smith, A. M.; Quick, T. J.; St. Peter, R. L. *Biol. Bull.* **1999**, *196*, 34–44.
- (22) Flammang, P.; Ribesse, J.; Jangoux, M. *Integr. Comp. Biol.* **2002**, *42*, 1107–1115.
- (23) Cleary, G. W.; Feldstein, M. M.; Beskar, E. Business Briefing: Pharmatech 2003, Technology & Services Section, May 2003. Online at <http://www.bbriefings.com/download.cfm?fileID=608> (accessed Nov 2004).
- (24) Callow, A.; Crawford, S. A.; Higgins, M. J.; Mulvaney, P.; Wetherbee, R. *Planta* **2000**, *211*, 641–647.
- (25) Gosline, J.; Lillie, M.; Carrington, E.; Guerette, P.; Ortlepp, C.; Savage, K. *Philos. Trans. R. Soc. London B*, **2002**, *357*, 121–132.
- (26) Combie, J. Adhesives & Sealants Industry, Cover Article 6 Feb, 2003. Online at http://www.adhesivesmag.com/asi/cda/articleinformation/coverstory/bnpcoverstoryitem/0,,101154,00+en-uss_01dbc.html, accessed Nov 2004.
- (27) Doolittle, R. F. *Of URFs and ORFs: A primer on how to analyze derived amino acid sequences*; University Science Books: Mill Valley, California, 1986; p 55.
- (28) Tatham, A. S.; Shewry, P. R. *Trends Biochem. Sci.* **2000**, *25*, 567–571.
- (29) Kivirikko, K. I.; Myllylä, R.; Pihlajaniemi, T. In *Post-Translational Modifications of Proteins*; Harding, J. J., Crabbe, M. J. C., Eds.; CRC Press: Boca Raton, FL, 1992; pp 1–51.
- (30) Burzio, L. O.; Burzio, V. A.; Silva, T.; Burzio, L. A.; Pardo, J. *Curr. Opin. Biotechnol.* **1997**, *8*, 309–312.
- (31) Deming, T. J. *Curr. Opin. Chem. Biol.* **1999**, *3*, 100–105.
- (32) Waite, J. H. *Ann. N.Y. Acad. Sci.* **1999**, *875*, 301–309.
- (33) Waite, J. H. *Integr. Comp. Biol.* **2002**, *42*, 1172–1180.
- (34) Graham, L. D.; Glattauer, V.; Ramshaw, J. A. Unpublished data.
- (35) Frost-Mason, S.; Morrison, R.; Mason, K. In *Amphibian Biology*; Heatwole, H., Barthalmus, G. T., Eds.; Surrey Beatty: Chipping Norton, Australia, 1994; Vol.1, pp 64–97.
- (36) Naldrett, M. J.; Kaplan, D. L. *Mar. Biol.* **1997**, *127*, 629–635.
- (37) Kamino, K.; Inoue, K.; Maruyama, T.; Takamatsu, N.; Harayama, S.; Shizuri, Y. *J. Biol. Chem.* **2000**, *275*, 27360–5.
- (38) Graham, L. D. Biological adhesives from nature. In *Encyclopedia of Biomaterials and Biomedical Engineering*; Wnek, G., Bowlin, G., Eds.; Marcel Dekker: New York, 2005; online update, in press. Encyclopedia online at <http://www.dekker.com/sdek/issues~db=enc~content=t713172959>.
- (39) Stanley, M. S.; Callow, M. E.; Callow, J. A. *Planta* **1999**, *210*, 61–71.
- (40) Smith, A. M.; Morin, M. C. *Biol. Bull.* **2002**, *203*, 338–346.
- (41) DeMoor, S.; Waite, J. H.; Jangoux, M.; Flammang, P. *Mar. Biotechnol.* **2003**, *5*, 45–57.
- (42) Jin, H.-J.; Kaplan, D. L. *Nature* **2003**, *424*, 1057–1061.
- (43) Zhou, C.-Z.; Confalonieri, F.; Medina, N.; Zivanovic, Y.; Esnault, C.; Yang, T.; Jacquet, M.; Janin, J.; Dugué, M.; Perasso, R.; Li, Z.-G. *Nucleic Acids Res.* **2000**, *28*, 2413–2419.
- (44) Vollrath, F.; Knight, D. P. *Nature* **2001**, *410*, 541–548.
- (45) Valluzzi, R.; Winkler, S.; Wilson, D.; Kaplan, D. L. *Philos. Trans. R. Soc. London B* **2002**, *357*, 165–167.
- (46) Debelle, L.; Alix, A. J.; Wei, S. M.; Jacob, M. P.; Huvenne, P.; Berjot, M.; Legrand, P. *Eur. J. Biochem.* **1998**, *258*, 533–539.
- (47) Urry, D. W.; Hugel, T.; Seitz, M.; Gaub, H. E.; Sheiba, H. E.; Dea, J.; Xu, J.; Parker, T. *Philos. Trans. R. Soc. London B* **2003**, *357*, 169–184.
- (48) Hayashi, C. Y.; Lewis, R. V. *J. Mol. Biol.* **1988**, *275*, 773–784.
- (49) Aggeli, A.; Bell, M.; Keen, J. N.; Knowles, P. F.; McLeish, T. C. B.; Pitkeathly, M.; Radford, S. E. *Nature* **1997**, *386*, 259–262.
- (50) Ozbas, B.; Kretsinger, J.; Rajagopal, K.; Schneider, J. P.; Pochan, D. J. *Macromolecules* **2004**, *37*, 7331–7337.
- (51) Peng, Y.; Glattauer, V.; Graham, L. D.; Vaughan, P. R.; White, J. F.; Werkmeister, J. A.; Tyler, M.; Ramshaw, J. A. M. 7th World Biomaterials Congress, May 2004, Sydney, Australia; Poster THU2.060, abstract 1654.

BM050335E